Journal of Ceramic Processing Research. Vol. 25, No. 3, pp. 365~374 (2024)
(Received 26 February 2023, Received in revised form 30 March 2024, Accepted 8 April 2024)
https://doi.org/10.36410/jcpr.2024.25.3.365

J O U R N A L O F
Ceramic Processing Research

Modification of 2205 duplex stainless steel properties through solution heat treatment and surface enhancement with sol gel coatings for biomedical applications

Alaa Khalid Abd Al-reda*, Nawal Mohammed Dawood and Shaima'a J. Kareem
University of Babylon, College of Materials Engineering, Iraq

Heat treatment and surface modification with a layer of titania (TiO_2) and TiO_2-SiO_2 composite coating with varying compositions (from 0 to 40 mol% SiO_2) by sol gel dip coating technique on 2205 duplex stainless steel. As a precucer for titania, titanium isopropoxide, for silica, tetraethyl orthosilicate were used and hydrochloric acide as a catalyst, ethanol as solvent and diethanolemaine as dispersant microstructure analysis after heat treatment was studied SEM, XRD. The FESEM was used to analyses the coating's morphology microscopically and EDS. Also surface roughness and contact angle were evaluated. The corrosion resistance of DSS in Ringer's solution was investigated by photodynamic polarization. The study aims to assess DSS's capabilities for bio applications to replace austenitic grades. The heat treatment gives a balanced microstructure and no precipitation of secondary phases. The sol-gel approach proved effective in producing a homogenous and dense layer of titania and composite coatings, increased roughness after coating therefore reducing the contact angle and making it more hydrophilic, making it suitable for bio application with the nano composite coating producing the best results. It is due to its smooth surface increase film thickness and results showed that sol-gel composite coatings greater bioactivity and enhanced the corrosion resistance of DSS substrates, with the highest improvement percentage (91.95%) at C2 specimen.

Keywords: Duplex stainless steel, Heat treatment, TiO_2-SiO_2, Sol gel, Coating.

Introduction

Duplex stainless steels (DSS) have a microstructure that contains almost equal proportions of ferrite and austenite phases, resulting in a beneficial combination of mechanical qualities such as strength, ductility, and corrosion resistance [1, 2]. While the presence of the austenite phase may improve the toughness of ferritic stainless steels, the ferrite phase enhances the yield strength and stress corrosion cracking (SCC) of austenitic stainless steels. DSS is regarded as an alternative material to austenitic stainless steel for usage in the medical industry since it minimizes or eliminates the detrimental effect of allergic responses when Ni is released, making it a superior biomaterial than austenitic stainless steel. More than 90% of implants fail due to the low crevice and pitting corrosion resistance of 316L stainless steel in the human body [3]. Surface modification of a prosthetic device often improves corrosion resistance and biocompatibility. Several surface modification approaches are used to increase biocompatibility in physiological media. Plasma ion implantation [4], laser surface alloying [5], physical and chemical vapour deposition [6], and thermal oxidation [7] are a few examples. Furthermore, each process has its own limits, which, with their complicated operating procedures, affect the performance of the modified surface a simple approach for physically and chemically evenly covering bio implants with a sol-gel-derived ceramic coating is used. Recent advances in sol-gel technology have resulted in the effective application of sol-gel-derived coatings onto metallic implants with desirable qualities for orthopedic applications [8, 9]. The sol-gel manufacturing process is a potential approach for producing bioactive materials for biomedical purposes. The increased interest in sol-gel materials stems from their capacity to create close contact with surrounding tissues, resulting in a strong chemical interaction [10]. Titanium dioxide (TiO_2)-based coatings have a variety of applications in biomedical engineering due to their great mechanical, osteoconductive and corrosion-resistant properties. TiO_2 coating's chemical stability, nontoxicity, and biocompatibility have led to suggestions that it replace the biomedical implant coatings that are now in use. Thin-film titanium dioxide (TiO_2) coatings are widely recognised for their capacity to enhance cellular viability, an essential component of biocompatibility [11]. However In addition to having anti-corrosion qualities, silica (SiO_2) is a very active substance that encourages the growth of osteoblasts, which are a kind of bone cell, and causes the creation of hydroxyapatite [12]. In vitro and in vivo tests have shown the biocompatibility of the TiO_2-SiO_2-sol-gel

*Corresponding author:
Tel : 07823924893
E-mail: alaakhalid9666@gmail.com

coatings. [10] In the fields of optics [13], nano bio composites [14], biomaterials [15], and self-cleaning materials [16] sol-gel coatings are extensively researched S.M.A. Shibliet et al. (2008) In this research, TiO_2 layer was deposited on titanium substrate by sol gel method silica was added in specific ratio a TiO_2-SiO_2 mixed oxide was created the result show that titania has anatase structure, the coating adhesion and corrosion resistance were improved by silica added [17]. Virpi äritalo et al. (2010) studied The development of low-temperature sol-gel coatings for shape memory metal (NiTi) TiO_2-SiO_2 coatings with silica contents ranging from (0 to 30) mol%. Also studied by using Polyethylene glycol (PEG) to prepare the coatings layer the results show the novel low temperature sol-gel TiO_2-SiO_2 90/10 coating was found to perform equally well with traditional high temperature TiO_2 coating in rat subcutaneous environment after a four weeks implantation period [10]. Mehtap Demirel et al. (2018) Using the sol-gel process, HA powders with varying particle sizes (0.68, 1.2, and 2.4 μm) were created. According to test results, the HA-based biograft sample's microhardness and compressive strength declined as particle size increased. Biografts synthesised at smaller powder particle sizes, such as 0.68 μm and 1.2 μm, showed the highest cell viability [18]. Fouzia Saadaoui et al. (2019) CuO thin films were deposited using the sol gel spin-coating process on microscope glass substrates and annealed at two different temperatures. The results reveal that the average crystallite size increased from 28.06 to 37.68 nm with the increase of both thickness and annealing temperature [19]. Reza AHMADI et al. (2021) created layer of nano composite (HAp (hydroxyapatite), TiO_2, and Al_2O_3) on 316L stainless steel by sol gel method to improve corrosion resistance and biocompatibility of 316L SS (Stainless Steel) metal implants. As a result, HAp + 30%wt (TiO_2 + Al_2O_3) coatings have superior biocompatibility, adhesion strength, and corrosion resistance than other coatings, indicating that this enhanced coating has better qualities than hydroxyapatite coatings [20]. Pankaj Kuma et al. (2021) In this research, titanium dioxide (TiO_2) thin film coated on stainless steel (SS316L) substrate to studied surface Bone integration. According to the results, specimen made with the highest pre-cursor concentration has appear lower roughness characteristics [21].

The aim of this work is to obtain a protective coating of TiO_2, TiO_2-SiO_2 by the sol gel method (dip coating technique) on duplex stainless steel substrates after heat treatment and investigate their surface morphology, phase composition ,corrosion behavior in ringer solution, and chemical bioactivity in simulated body fluid.

Experimental Procedure

In this work, titania (TiO_2) and composite coating (TiO_2-SiO_2) sol-gel-generated coatings were dip-coated on 2205 duplex stainless steel (DSS). After heat treatment, the substrate is coated. The heat treatment was performed at 1100 °C for 15 minutes, then quenched in cold water ray fluorescence (XRF) type (DS-2000) used for the chemical analysis as showed in Table 1.

Using silicon carbide sheets with grits of 220, 400, 600, 800, 1000, and 1200, DSS substrates were ground then use ultrasonically cleaning by immersion in acetone for five minutes and ethanol for five minutes, and dried using in hot air.

The TiO_2 coating films were formed by immersing the substrate in $Ti(OH)_4$ precursor solution which prepared by dissolving titanium tetra-isopropoxide (TTIP) using a precursors for TiO_2 in ethanol, raising the stirring temperature to 40 °C, stirring for 30 minutes, and then mixing with distilled water, drops of hydrochloric acid (HCl, 37%) were used as catalyst, and triethanol amine used as a dispersant in the molar ratio TTIP : ethanol : water : HCL = 1 : 27 : 15 : 1. Before dipping to get sol (A) the sol was aged for 24 hours. In order to develop the SiO_2 coating, tetraethyl orthosilicate (TEOS, $Si(OC_2H_5)_4$), using as precursors for SiO_2 ethanol and distilled water were added in the $Si(OH)_4$ sol, following molar ratios: $EtOH : H_2O : TEOS$ = 1.8 : 18 : 1. then put on a magnetic stirrer while keeping a constant temperature. To produce sol (B), the stirring temperature was adjusted to 30 °C for 30 minutes. TiO_2-SiO_2 composite coating films, were prepared by mixing The sols with different volume ratios, as shown in Table 2, Stirring was done for one hour at constant temperature, then aged for 24 hours before dipping process.

Table 1. Chemical composition of 2205 DSS (wt %).

Elements	C	Si	P	S	Cr	Mo	Ni	Al
Weight %	0.0271	0.33	0.0270	0.0005	23.46	3.44	5.22	0.0047
Elements	Cu	Co	Nb	Ti	V	W	Mn	Fe
Weight %	0.105	0.105	0.0178	0.0116	0.129	0.0477	1.34	Bal

Table 2. volume ratios of mixing sols.

Specimens code	A	B	C1	C2	C3	C4
Volume ratios of mixing sols	BASE	100%TIO_2	90%A-10% B	80% A-20%B	70%A-30%B	60 %A-40%B

Table 3. The chemical compositions of SBF solution.

Component	NaCl	$NaHCO_3$	KCl	$K_2HPO_4{\cdot}3H_2O$	$MgCl_2{\cdot}6H_2O$
Concentration	8.035 g	0.355 g	0.225 g	0.231 g	0.311 g
Component	1.0 M HCl	$CaCl_2$	Na_2SO_4	$((HOCH_2)_3CNH_2)$	1.0 M HCl
Concentration (g/l)	39.0 ml	0.292 g	0.072 g	6.118 g	Appropriate amount for adjusting pH~7.4

Specimens were immersed in the soles for 30 seconds and then withdrawn at a rate of 80 mm/min at ambient environment. The coating technique was repeated five times after natural drying in air for 1 minute, and then the substrates were dried at 80 °C for 1 hour and calcined at 600 °C for 1 hour at a heating rate of 5 °C/min.

Characterization tests

Microstructure examination achieved by using carpenter etching solution [22]. After the etching process, specimens were washed with water and dried [22]. The morphology of the substrate specimens before and after heat treatment was investigated using an optical microscope model (BEL PHOTONICS), and examined microscopically with a (JEOL-JSM) scanning electron microscope (SEM). The phases of the substrate were studied with an X-ray diffract meter (XRD) model (Lab X 6000, Shimadzu, Japan origin). CuKα radiation at 40 KV and 7 mA was employed as the X-ray source in the XRD test, and the scanning were Ø from 30º to 80º. The field emission scanning electron microscope (FE-SEM) model (Axia Chemise) was used to analyses the coating's morphology microscopically, and energy dispersive spectroscopy (EDS) was employed to look into the elemental composition. and both before and after coating, the surface roughness was assessed. Surface Roughness Tester Type (TR200, SaluTron, produced in Germany) was used to measure it. Wettability test The water contact angles (WCA) were obtained by measuring the contact angle (θ) of a droplet on a solid surface using ringer solution, The optical contact angle equipment type (CAM 11O-O4W), which was attached to a CCD camera, was used to measure the contact angle.

Corrosion test

Tests for electrochemical corrosion specimens before and after coating using potentiodynamic measurements in "Ringer's solution" at 37 °C Chemical Ingredients (NaCl (8.06 g/l), KCl (0.30 g/l), $CaCl_2{\cdot}2H_2O$ (0.33 g/l)) and PH (5-7.5) using a potentiostat/galvanostat type (MLab Bank Elektronik, Germany). Three electrodes made up the corrosion cell: a saturated calomel electrode (SCE), a platinum rod serving as the counter electrode, and the sample acting as the working electrode. The corrosion rate (CR) was calculated by using Faraday's law in mpy units according to ASTM G102-89.

Bioactivity test

The Experiments were performed in vitro by soaked the uncoated and coated specimens were soaked in 25 ml of simulated bodily fluid (SBF) was prepared by dissolving reagents as shown in Table 3 after soaked in SPF solution for four weeks at 37 °C.

Results and Discussion

Effect of solution treatment on microstructure

The effect of solution treatment on the microstructure and morphology of 2205 duplex stainless steel is depicted in Figs. 1 and 2 using optical micrographs and SEM images. Only two secondary phases are evident in the untreated specimen of 2205 duplex stainless steel, according to the micrograph: ferrite (α) and austenite (γ) [23]. the photograph shows that When compared to austenite, ferrite appears darker. The micrograph following heat treatment makes this evident. The

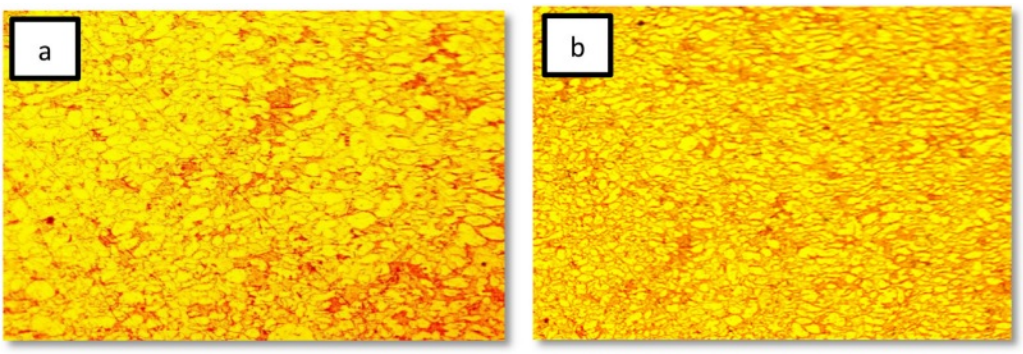

Fig. 1. Optical micrographs of 2205 DSS. (a) Untreated specimen (b) treated specimen

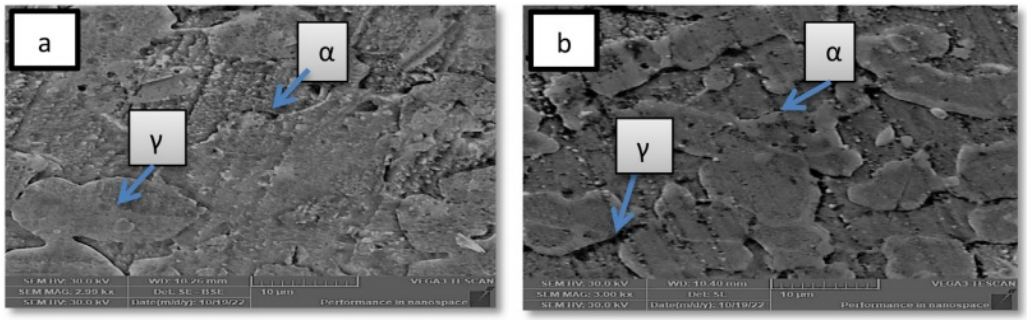

Fig. 2. SEM morphologies of 2205 DSS. (a) Untreated specimen (b) treated specimen

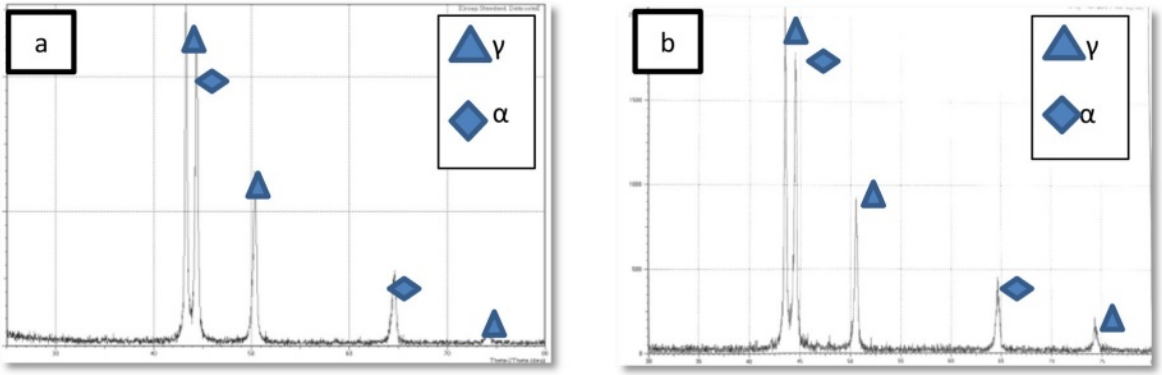

Fig. 3. X-Ray diffraction pattern of 2205 DSS. (a) Untreated specimen (b) treated specimen

austenite was found dispersed throughout the ferritic matrix as acicular and lamella islands, with no signs of secondary phases [24]. It was discovered that the matrix had a larger distribution of austenite with a homogenous shape. This heat treatment is required to remove secondary phases, balance phase fractions, and relieve any residual stresses from the manufacturing process. it can be seen from (Fig. 2b) that microscopic structure was homogeneous after heat treatment in addition, the grain size has become smoother than before treatment, and this is useful for improving the properties agree with [24, 25].

XRD is used to determine the phases of 2205 DSS samples before and after heat treatment, were shown in Fig. 3a and Fig. 3b obviously, the sigma phase and other secondary phases did not appear, and the peaks in diffraction patterns belong to ferrite and austenite phase these result similar to [24] it is clear that the X-ray diffraction results were confirmed by optical and scanning electron microscops images.

Field Emission Scanning Electron Microscopy (FE-SEM)

Figure 4 displays FE-SEM images of TiO_2 and (TiO_2-X SiO_2) composite for coating layers coated on 2205 DSS surface by sol gel method with cross-section. cross section image show a regular coating layer structure and difficult to detect interface between coatings and substrates indicates a strong adhesion between coating and substrate the thicknesses of nano composite film for specimens (C1, C2, C3, and C4) are higher than the thickness of TiO_2 coating (B) specimen. The B specimen thickness coating (1.73 μ) and for (C1, C2, C3, C4) (2.68, 3.55, 3.56, 4.43) μ, respectively. The images show the substrate coated with titania. The surface is totally covered with pure TiO_2 coating, consisting mainly of nano sized particles and different irregular clusters arranged together to achieve good adhesion on the substrate with particles size (173.131 nm-96.292 nm), porous structure the size range of pores (161.329 nm-157.421 nm) this result agree with [26] and demonstrate the influence of adding silica particles to the TiO_2 matrix on the DSS surface. That, as compared to a TiO_2 coating, the inclusion of silica with various percentages (10-40)% mol produces surfaces with greater uniformity and smoother surface. The coating's higher silica concentration leads to smoother surfaces smaller particles and low porosity, which increases coating thickness. Where 10% molar ratio amounts of SiO_2 decrease size of particles to (108.7-43.78) nm as well as decrease the amount of pores with size range (146.61-135.151) nm and reduce the particles range size to (29.54-26.27) nm, (60.634-22.059) and (56.654-15.36) nm reduce amount and the size of the pores to (143.568-67.48) nm (44.271-39.597) nm, and (31.644-29.629) nm respectively for C1, C2, C3, C4 specimens respectively. The silica

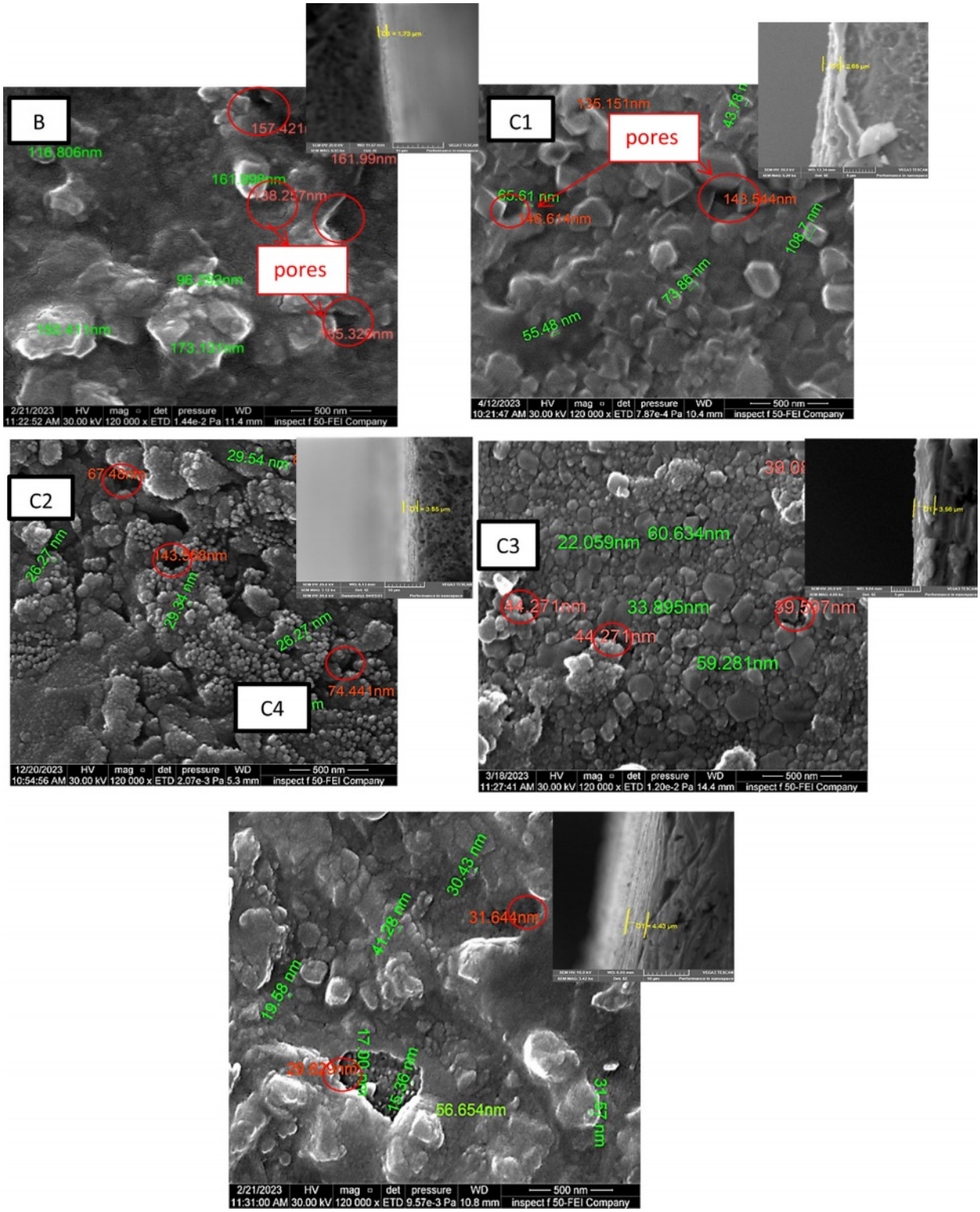

Fig. 4. FE-SEM images of coating Specimenes.

contributed to change the property of surface in the by reducing surface roughness in the coating uniformity. and the cracks have mostly been eliminated agree with [25]. In medical applications the presence of pores is necessary for ossointegration at the same time, many pores can cause risk resulting from the large amount of body illiquid . there for it is neccessary to obtain the best mechanical and biological performance, coating porosity levels must be carefully adjusted agree with [27, 28].

Energy dispersive spectroscopy (EDS)

EDS analysis revealed the presence of prominent

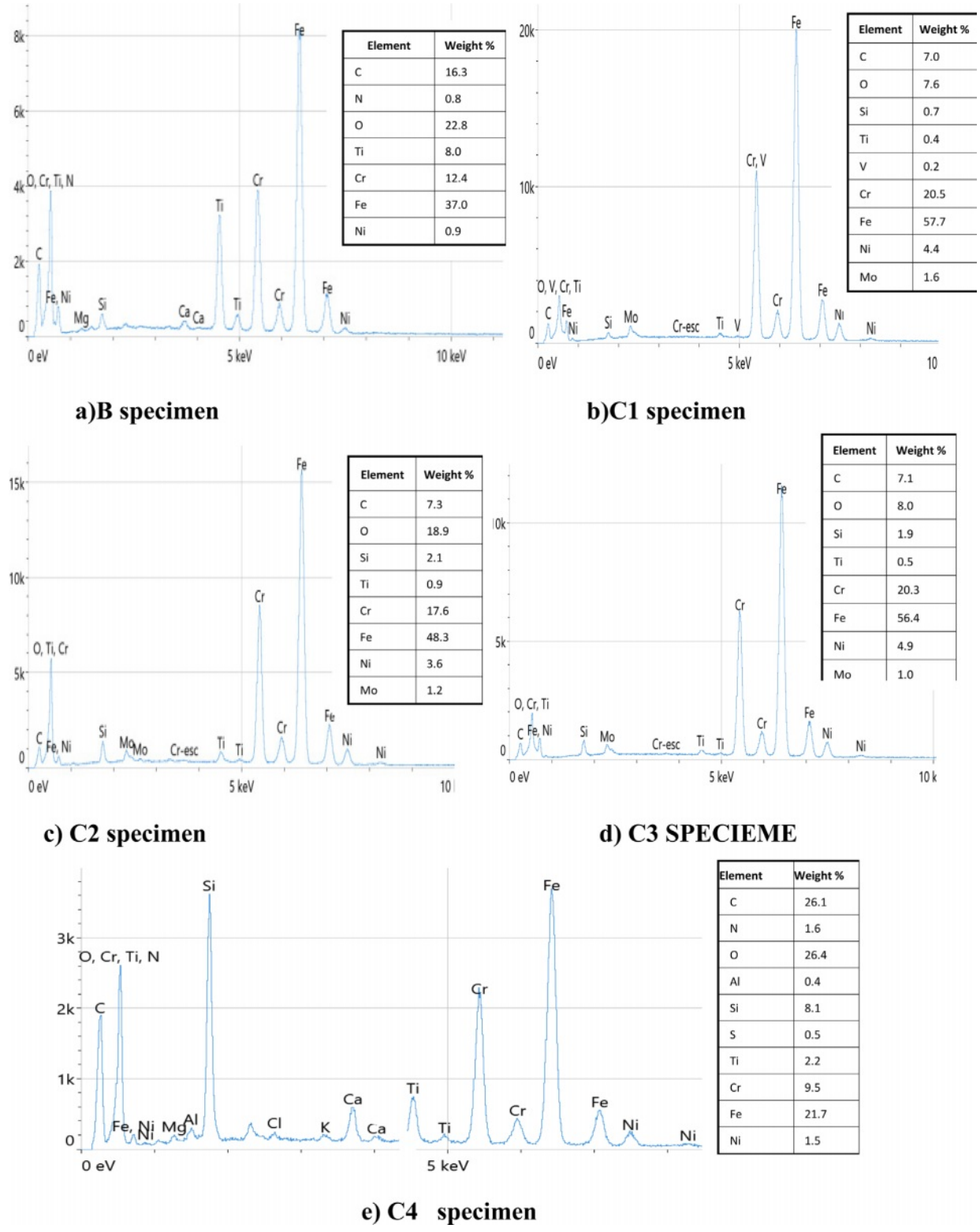

Element	Weight %
C	16.3
N	0.8
O	22.8
Ti	8.0
Cr	12.4
Fe	37.0
Ni	0.9

Element	Weight %
C	7.0
O	7.6
Si	0.7
Ti	0.4
V	0.2
Cr	20.5
Fe	57.7
Ni	4.4
Mo	1.6

Element	Weight %
C	7.3
O	18.9
Si	2.1
Ti	0.9
Cr	17.6
Fe	48.3
Ni	3.6
Mo	1.2

Element	Weight %
C	7.1
O	8.0
Si	1.9
Ti	0.5
Cr	20.3
Fe	56.4
Ni	4.9
Mo	1.0

Element	Weight %
C	26.1
N	1.6
O	26.4
Al	0.4
Si	8.1
S	0.5
Ti	2.2
Cr	9.5
Fe	21.7
Ni	1.5

Fig. 5. EDS Results of a) B b) C1 c) C2 d) C3 e) C4 specimen.

elements in the coatings. The elemental composition of the TiO_2 and (TiO_2-SiO_2) composite coating deposited on the duplex stainless steel substrate are shown in Fig. 5. It can be seen that the coatings include the three primary components (Ti, Si, and O). These components are present, which assertion that the coating on the 2205 DSS substrate was successfully formed agree with [26]. Higher silica concentrations were found in specimens with composite TiO_2-SiO_2 coatings. This shows that the outermost surface of these coatings is enriched in silica.

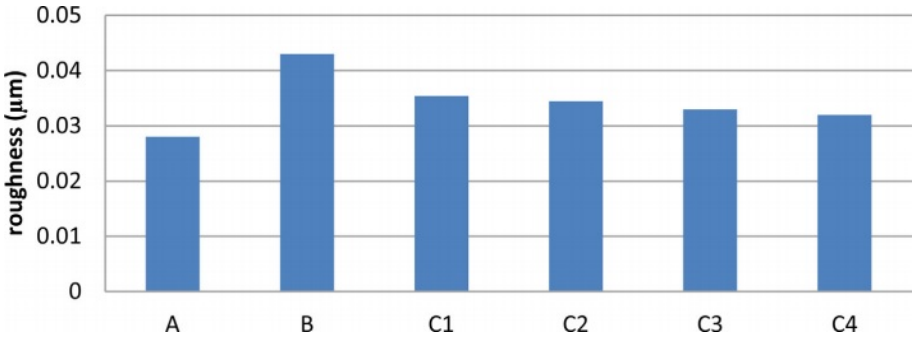

Fig. 6. Roughness result of the Uncoated and Coated specimens.

The somewhat higher hydrolysis rate of TTIP compared to TEOS may account for the little discrepancy between the Si/Ti ratio in the SiO_2-TiO_2 films and the sols mixing ratio. As a result, the solution's Ti concentration is a bit lower than the initial mixing ratio, causing a minor Ti deficit in the finished film agree with [27, 29].

Surface Roughness

The roughness of the coated and un coated specimen were shown in Fig. 6 which Cleary that roughness increases relative to the surface without coating. The results showed that the titania coating specimen was rougher, and after adding silica to TiO_2, the surfaces became smoother with the increase in the amount of SiO_2, but rougher than substrate without coating. The addition of silica leads to very significant changes in all surface coating properties, which makes the surface roughness of the coating decrease for TiO_2, composite coating with preferred homogeneity, which helps to improve the surface compared with TiO_2 coating. TiO_2 coating has a surface with the highest roughness among specimens however, without proper mechanical strength, the high roughness would not be worthwhile [27]. By measuring surface roughness, of TiO_2-SiO_2 composite coatings are the best choice with compare with TiO_2. Increased surface roughness than substrate without coating has been shown to facilitate fast osteoblast cell attachment to the implant surface, potentially leading to a large increase in the area of the implant that makes contact with the bone. On the other side, enhanced bacterial adherence results from increasing surface roughness therefore bio composite coatings are the best choice among others specimens agree with [30].

Contact Angle Measurements

Contact angle is a measure of wettability and surface free energy a small contact angle indicates excellent wettability, whereas a large contact angle indicates poor wettability. Furthermore, good wettability is an significant characteristic for biomaterials to attach to tissue. The value of contact angle as shown in Fig. 7 for the coated and uncoated specimens show different results, showing the extent to which this layer is hydrophilic or hydrophobic inside the human body. The surface of the uncoated specimen has a higher aqueous contact angle of 103°, which indicates a hydrophobic surface compared to the coated samples. The contact angle decreased to 39° for specimen B and (44°, 54°, 69°, 76°) for specimens (C1, C2, C3, C4) respectively. The reduced contact angle may be attributed to the effect of surface texture (surface roughness) and other biocompatible phases TiO_2 (rutile and anatase) is formed during calcination

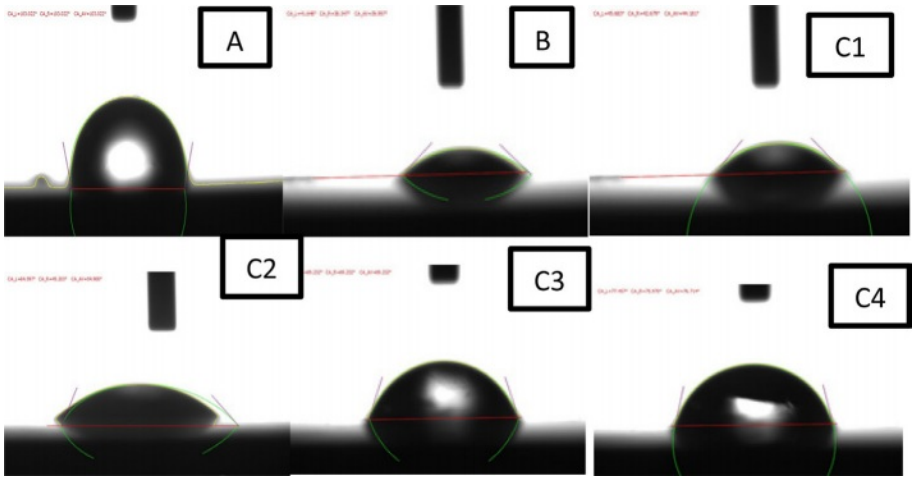

Fig. 7. Results contact angles of the Coated and Uncoated specimens in ringer solution.

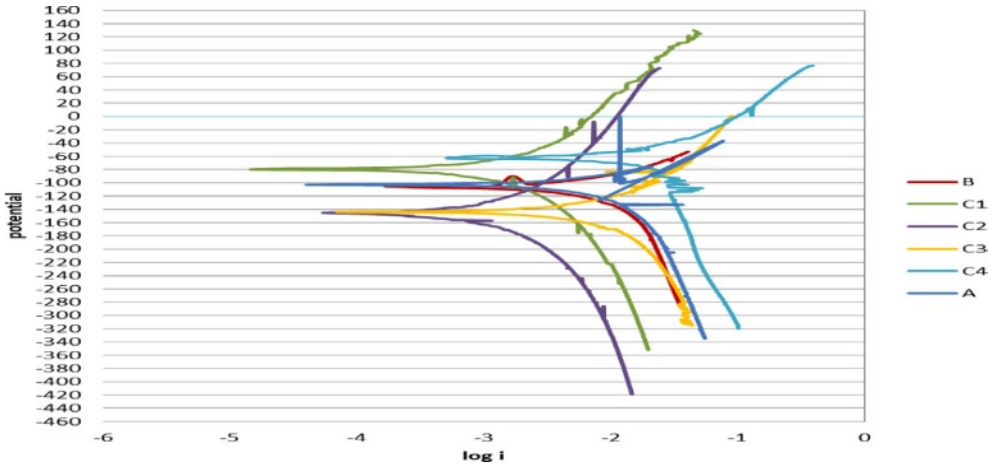

Fig. 8. Potentiodynamic polarization curves of coated specimens and uncoated in Ringer solution at 37 ºC.

also adding silica to titania TiO_2 coating incorporate of formation of a more bioactive phase in the composite bio coatings, as these phases provide a synergistic effect to make the surface more hydrophilic. So, the specimens after coating have the best wettability because of their excellent hydrophilic nature agree with [10].

Corrosion Test

Figure 8 shows the potentiodynamic polarization curves of uncoated 2205 DSS specimens and coated in ringer solution at 37 ºC. Table 4 demonstrate the corrosion parameters extrapolated from these curves. Corrosion potential (E_{Corr}), corrosion current (i_{Corr}), corrosion density (I_{Corr}), corrosion rate CR(mpy) and Improvement rate are the parameters for corrosion. When i_{Corr} is reduced, the specimens' corrosion resistance increases. For the substrate, i_{Corr} was about (11 µA) and then decreased to (5 µA) for TiO_2 while for TiO_2-SiO_2 composite coating the current reach to (1.03, 0.904, 2.21, 2.80) µA for specimens (C1, C2, C3, C4) respectively the results showed that the substrate have the higher corrosion current. After coating, it can be observed that the corrosion current of specimens decreases. This means that the coating provides a protective layer on the alloy surface, and the low porosity is beneficial because it reduces the path of the Ringer solution to reach the surface of the substrate and thus increases the resistance to corrosion after coating of the specimens, as result corrosion rate reduce the corrosion rate and enhance resistance against corrosion and oxidation as a results the corrosion rate shifts towards the lower value after coated with single (TiO_2) and composite (TiO_2-xSiO_2) coating as shown in Table 4. These results proved that ceramic coating played a major role reducing the corrosion rate in a biological solution the reason is due to TiO_2 coating on 2205 DSS was uniform and compact and its adhesion to substrate was very good another advantage of TiO_2 coating is more biocompatibility [31] for specimen with composite (TiO_2-xSiO_2) coating, it showed A significant decrease in current density as compared with DSS substrate and pure (TiO_2) coated specimen the presence of (TiO_2-10%SiO_2) composite coating increase the corrosion resistance by decreasing the current densities from (3.187) µA/cm^2 for the B specimen to (0.583) µA/cm^2 for C1 specimen the reducing in the current density become more significant for C2 specimen (TiO_2-20%SiO_2) ceramic composite coating which has the best improvement rate in corrosion resistance reached to (91.95%) metals coated with composite ceramic oxide using sol gel method attracted more interest from researcher recently because these coating combined between bioactivity and biocompatibility properties agree with [32] especially coating SiO_2 which showed a significant resistance to corrosion with more biocompatibility surface due the

Table 4. the electrochemical Parameters calculated using potentiodynamic polarization of coated specimens and uncoated in Ringer solution at 37 ºC.

Sample code	E (mv)	I corr. (µA)	I corr. (µA/cm^2)	CR (mpy)	Improvement rate
A	-104.5	11.42	6.465	1.690	
B	-103.8	5.63	3.187	0.850	49.70%
C1	-82.2	1.03	0.583	0.155	90.82%
C2	-147.4	0.904	0.511	0.136	91.95%
C3	-142.1	2.21	1.251	0.333	80.29%
C4	-60.7	2.80	1.585	0.409	75.02%

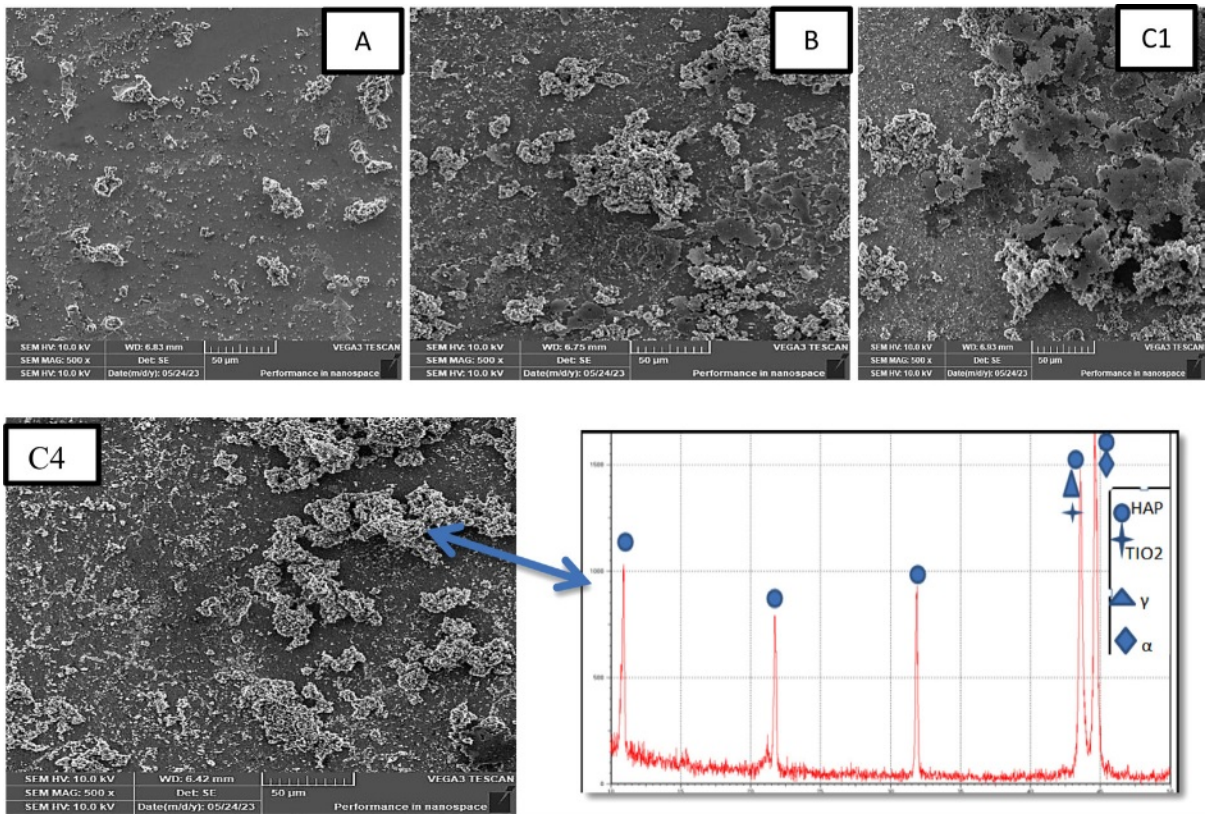

Fig. 9. Images of the surface morphology of the specimens before and after coating after immersing in SBF after 30 days and X-Ray diffraction pattern for HAP layer.

presence of SiO_2 these result were confirm by many researchers agree with [28, 33].

Bioactivity

SEM images after bioactivity test, which achieved by immersion of coated and un coated specimens in SPF solution for 30 days are shown in Fig. 9. It is noted that the coated and un coated surface covered with a layer of hydroxyapatite with spherical particles. however, the hydroxyapatite layer formed on all coated specimen was larger and denser compared with un coated specimen. as the amount of immersion time increases, the amount of hydroxyapatite particles formed increases, and this helps us biologically since it can improve the ability for implants placed inside people's bodies to bind with their bones with which it was created more in the (TiO_2-SiO_2) composite film's due to the the presence of (Si-O-Si) bands on its surface, presence porosity, and nucleation sites (Si-OH) easier to develop, and promotes the Rapid apatite surface deposition. XRD graph of HAP layer formed on C4 are shown in Fig. 9 These calcium phosphate layer can improve Osseo integration agree with [28].

Conclusions

In this work, The most suitable heat treatment results in a balanced microstructure and no precipitation of secondary phases and sol-gel method was successful in creating a homogeneous and dense layer of titania and (TiO_2-SiO_2) bio composite coatings with varying SiO_2 contents (from 0 to 40% mol), and coated using a dip coating process on a duplex stainless steel substrate after heat treatment silica at various percentages produces surfaces with greater uniformity and smoother surface structures and It was found that ceramic films displayed improvements in the corrosion protection of substrates where the lowest value corrosion rate (0.136 mpy), and maximum improvement percentage (91.95%) are at specimen C2. Bioactivity tests revealed that composite films, which include Si-O-Si bands on their surface and are porous in design, had higher bioactivity. Based on all of these results, we may conclude that composite films have superior bioactivity qualities over TiO_2 films and uncoated substrates. As a result, it may be an excellent substrate in contact with live tissues.

Acknowledgements

The authors appreciate the assistance provided by the University of Babylon, Especially the laboratories of the Faculty of Materials Engineering.

References

1. C.R. de Lima Lessa, D. Martinazzi, A.P. Figueiredo,

G.V.B. Lemos, and A. Reguly, Mater. Sci. Tech. 35[4] (2019) 1161-1172.
2. A. Fedorov, A. Zhitenev, D. Strekalovskaya, and A. Kur, Mater. Proc. 3[1] (2021) 4.
3. S.M. Yang, Y.C. Chen, Y.T. Pan, and D.Y. Lin, Mater. Sci. Eng:C. 63[1] (2016) 376-383.
4. S. Mandl and B. Rauschenbach, Surf. Coat. Technol. 156[1-3] (2002) 276-283.
5. R. Singh, M. Martin, and N.B. Dahotre, Surf. Eng. 21[4] (2005) 297-306.
6. W.S. O'Shaughnessy, M. Gao, and K.K. Gleason, Langmuir. 22[16] (2006) 7021-7026.
7. P. Galliano, J.J.de Pamborenea, M.J. Pascud, and A. Duran, J. Sol-Gel Sci. Techn. 13[1-3] (1998) 723-727.
8. X. Liu, P.K. Chu, and C. Ding, Mater. Sci. Eng. 47[3-4] (2004) 49-121.
9. J. Gallardo, A. Duran, and J.J. de Damborenea, Corros. Sci. 46[4] (2004) 795-806.
10. V. Meretoja, T. Tirri, S. Areva, J. Timo, J. Tuukkanen, A. Rosling, and N. Timo, Mat Sci Eng. 1[03] (2010) 118-126.
11. X. Zhao, H. Cao, J. You, X. Cheng, Y. Xie, H. Cao, and X. Liu, Appl. Surf. Sci. 355 (2015) 999-1006.
12. A. Śmieszek, A. Donesz-Sikorska, J. Grzesiak, J. Krzak, and K. Marycz, J. Biomater. Appl. 29[5] (2014) 699-714.
13. P. Surekha, A.D. Varshney, E. Jerusha, B. Pant, and A.S. Rajesh, Mater. Today Proc. 62[4] (2022) 2034-2037.
14. P.E. Johnson, P. Muttil, D. MacKenzie, E.C. Carnes, J. Pelowitz, N.A. Mara, and C.J. Brinker, ACS nano. 9[7] (2015) 6961-6977.
15. I. Stambolova, S. Yordanov, L. Lakov, S. Vassilev, V. Blaskov, and B. Jivov, In Matec Web of Conferences. EDP Sciences 145[7] (2018) 05011.
16. S.R. Meher and L. Balakrishnan, Mat. Sci. Semicon. Proc. 26[1] (2014) 251-258.
17. S.M.A. Shibli and S. Mathai, J. Mater. Sci-Mater. M. 19[8] (2008) 2971-2981.
18. M. Demirel and B. Aksakal, J. Ceram. Process. Res. 19[1] (2018) 5-10.
19. F. Saadaoui, A. Rjeb, B. Akharkhach, A. Nfissi, and S. Sayouri, J. Ceram. Process. Res. 20[2] (2019) 139-142.
20. R. Ahmadi and A. Afshar, Surf. Coat. Technol. 405[3] (2021) 126594.
21. P. Kumar, A.K. Das, and S. Mohanty, Mater. Lett. 303[6] (2021) 130553.
22. A.S. Fedorov, A.I. Zhitenev, D.A. Strekalovskaya, A.A. Kur, and A.A. Alkhimenko, Metals. 11[11] (2021) 1750.
23. O.A. Olaseinde, J. Van der Merwe, and L. Cornish, Adv. Chem. Engineer. Sci. 4[1] (2014) 89-93.
24. A.S. Hammood, A.F. Noor, and M.T. Alkhafagy, Mater. Res. Express. 4[12] (2017) 126506.
25. A.S. Hammood, A.F. Noor, and M.T. Alkhafagy, J. Mater. Sci.: Mater. Med. 28[187] (2017) 1-11.
26. M.T. Mohammed and S.M. Hussein, Karbala Int. J. Mod. Sci. 6[2] (2020) 14.
27. V. Ääritalo, S. Areva, M. Jokinen, M. Lindén, and T.J. Peltola, J. Mater. Sci.: Mater. Med. 18[9] (2007) 1863-1873.
28. M.S. Dadash, S. Karbasi, M.N. Esfahani, M.R. Ebrahimi, and H. Vali, J. Mater. Sci.: Mater. Med. 22[4] (2011) 829-838.
29. L.L. Yang, Y.S. Lai, J.S. Chen, P.H. Tsai, C.L. Chen, and C.J. Chang, J. Mater Res. 20[11] (2005) 3141-3149.
30. N.J. Hickok, I.M. Shapiro, and A.F. Chen, J. Dent. Res. 97[1] (2018) 14-22.
31. D. Sidane, H. Khireddine, F. Bir, S. Yala, A. Montagne, and D. Chicot, Metall. Mater. Trans. A. 48[2] (2017) 3570-3582.
32. S.A.Z. Estekhraji and S. Amiri, J. Inorg. Organomet. Polym. Mater. 27[4] (2017) 883-891.
33. S.K. Tiwari, T. Mishra, M.K. Gunjan, A.S. Bhattacharyya, T.B. Singh, and R. Singh, Surf. Coat. Technol. 201[16-17] (2007) 7582-7588.